JOC The Journal of Organic Chemistry

Article

pubs.acs.org/joc

Synthesis of Molecular Seesaw Balances and the Evaluation of Pyridinium−π Interactions

Shinji Yamada,* Natsuo Yamamoto, and Eri Takamori

Department of Chemistry, Faculty of Science, Ochanomizu University, 2-1-1 Otsuka, Bunkyo-ku, Tokyo 112-8610, Japan

Supporting Information

ABSTRACT: A series of molecular seesaw balances **1**−**5** have been developed to measure the relative strength of pyridinium−π (cation−π) interactions. The cycloaddition of 1-azaanthracene and *o*-quinodimethane under microwave irradiation afforded the efficient synthesis of **1** and **5**. Introduction of substituents to the pyridine ring of balance **1** was achieved to produce **2**−**4** in good yields. Anion exchange of **1**·MeI afforded **1**·MeX with a variety of counteranions (X = Cl, Br, I, BF_4, PF_6, OAc). These balances adopt two distinct conformers, **A** and **B**, which are stabilized by a cation−π interaction and a π−π interaction, respectively. The conformer ratio was determined on the basis of the observed averaged ^3J coupling constants for H_1−C−C−H_2 by comparison with the boundary J_A and J_B values, which were estimated by applying the Carplus−Altona equation to the dihedral angles of the optimized conformers **A** and **B**. The effects of the solvent, substituent and counteranion on the ΔG values were elucidated using these molecular balances. Thermodynamic parameters obtained from a van't Hoff plot as well as the electrostatic potential maps for both conformers **A** and **B** of the molecular balances helped us to better understand the obtained results.

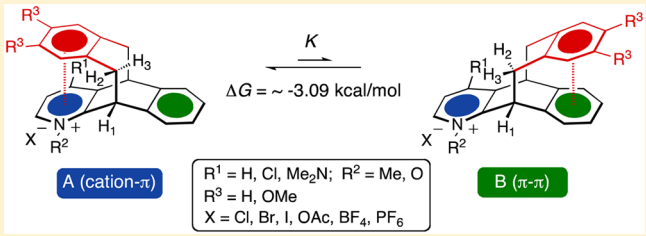

INTRODUCTION

It has been well documented that a cation−π interaction[1] plays a crucial role in molecular recognition in both biological[2,3] and supramolecular[4] systems. In addition, the importance of this interaction has recently emerged in the field of materials science.[3] For example, cation−π interactions between carbon nanotubes and ionic liquids[5] have received considerable attention with respect to changes in their physical properties. The properties of some polymers were drastically changed by the adhesion of cationic organic compounds.[6] As the strength of the interaction energy is generally larger than those of other aromatic interactions,[7] cation−π interactions affect not only large molecular systems but also small molecules. This makes it possible to use a cation−π interaction for stereoselective transformation[8] and crystal engineering.[9] Due to the increasing interest in the application in a broad range of fields within chemistry, the elucidation of the nature of cation−π interactions is of great importance in understanding their role in various molecular systems.

To elucidate the strength of the noncovalent interactions experimentally, various molecular balances have been developed,[10] in which a comparison of the two conformers existing in equilibrium can determine the energy difference between them. Two types of molecular balances have been reported: torsion and seesaw balances. After Wilcox et al. reported Tröger's base derivatives,[11] a number of torsion balances were developed.[12−19] On the other hand, there are only few reports on seesaw balances.[20−22] These balances are useful for the characterization of various noncovalent interactions, such as CH−π, NH−π, OH−π, π−π, and Ag−π as well as alkyl−alkyl interactions. However, there are only a limited number of approaches for assessing cation−π interactions using molecular balances.[18,21,24]

We designed a seesaw balance, a bidirectional molecular balance, for the comparative study of interaction energies between pyridinium−π and π−π interactions, as shown in Figure 1. This framework structure is closely related to our previously reported [4 + 4] photodimer of azaanthracene, in which the pyridine and benzene rings are close together.[23] We speculated that the removal of a pyridine ring from this dimer molecule would provide a new molecular balance. This balance consists of

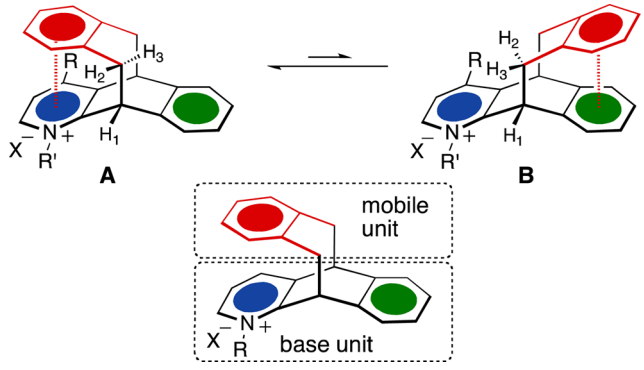

Figure 1. A seesaw balance for the quantification of pyridinium−π interactions.

Received: September 19, 2016
Published: November 3, 2016

DOI: 10.1021/acs.joc.6b02295
J. Org. Chem. 2016, 81, 11819−11830

azaanthracene- and quinodimethane-derived fragments; the azaanthracene-derived fragment possessing both aryl and pyridine rings forms the base unit of the balance, and the quinodimethane-derived fragment with a benzene ring is the mobile unit. The mobile unit connected to the base unit at C9 and C10 can move back and forth like a seesaw through its attraction to the benzene and pyridinium rings of the base unit. This balance has two conformers, **A** and **B**, which are stabilized by a cation−π interaction and a π−π interaction, respectively (Figure 1). An anthracene-based seesaw balance has also been developed by Motherwell and Aliev for the investigation of π-heteroatom interactions.[20]

This molecular balance has several advantages in the measurement of the interaction energies as follows: (1) there are only two distinct conformers, excluding undesirable conformational flexibility, (2) only face-to-face interactions are observed due to restricted motion of the mobile unit, and (3) as the two conformers show a high degree of symmetry, the direct comparison of the conformers is possible without the need for any reference compounds. In this paper, we report the synthesis of a series of molecular seesaw balances **1**−**5** as shown in Figure 2, together with the characterization of pyridinium−π interactions in which the solvent, substituent and counteranion affect the energies.

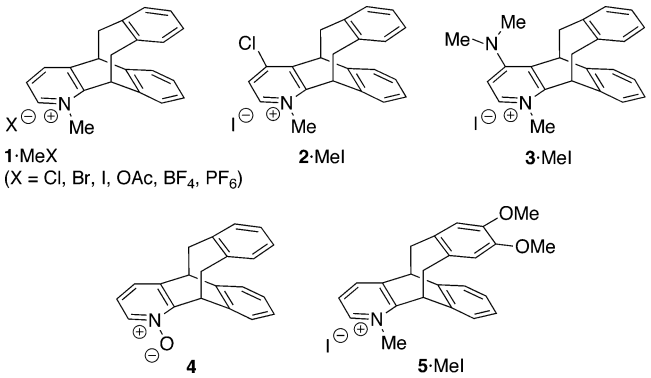

Figure 2. A series of molecular seesaw balances **1**−**5**. The *N*-Me forms are indicated for **1**−**3** and **5**.

RESULTS AND DISCUSSION

Synthesis of Molecular Seesaw Balances. A new molecular balance **1** was prepared by the reaction of 1-azaanthracene[23,25] and *o*-quinodimethane generated from the corresponding sulfone[26] or sultine[27] in situ, as shown in Scheme 1. The cycloaddition reaction was first carried out using reaction conditions similar to those for the addition of anthracene and *o*-quinodimethane reported by Shishido, Noyori and Nozaki.[28] Heating of azaanthracene and sulfone in diethyl phthalate at 270 °C for 3 h gave an adduct in 22% yield after removal of the solvent diethyl phthalate through hydrolysis, which was reported in a preliminary communication.[21] Considerable efforts to survey the reaction conditions were able to confirm that microwave irradiation is effective for improving the yield. Microwave irradiation of a toluene solution of **6** and **7** at 280 °C under 20 atom for 3 h produced **1** in 32% isolated yield (70% conversion yield). When the reaction time was increased to 4.5 h, the yield was improved to 48% yield (56% conversion yield). The merit of microwave synthesis of **1** lies in the fact that the reaction is carried out under high pressure, which is effective for addition reactions.[29] In addition, toluene can be used for the reaction at 280 °C, which allows much easier workup and purification compared to synthesis using diethylphtharate as a solvent.[28] The cycloaddition with sultine **9**, which was often used as a precursor of *o*-quinodimethane,[27,30] also afforded the adduct **1** in 32% yield under similar reaction conditions. The use of dimethoxyphenyl sulfone **8** as a precursor of the corresponding *o*-quinodimethane provided adduct **5** with two methoxy substituents at the mobile unit in 13% yield.

After the synthesis of **1** was established, we next examined the introduction of a substituent to the pyridine ring. Oxidation of **1** with MCPBA afforded *N*-oxide **4** in quantitative yield. Chlorination at the 4-position of the pyridine ring and deoxygenation were simultaneously performed using $POCl_3$[22] to give **2** in 70% yield. It is interesting to note that while chlorination of 3-substituted pyridine *N*-oxide produced 5- and 6-chloropyridines as major products,[31] the 4-chloropyridine was produced as a major product in this reaction. Next, our attempt at dimethylamination by the nucleophilic substitution of chloride **2** with 40% Me_2NH in THF yielded no product under reflux for 20 h. Inspired by a report demonstrating that MW irradiation is effective for the nucleophilic substitution of the pyridine ring with sterically hindered amines,[32] we next attempted to use MW synthesis. To our delight, microwave irradiation at 150 °C for 9 h significantly promoted the substitution reaction to give **3** in 61% yield.

Scheme 1. Synthesis of Molecular Balances 1−5

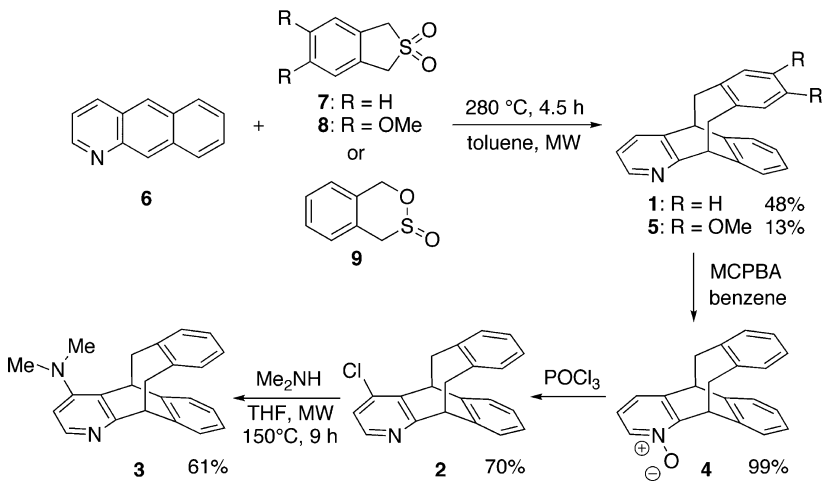

DOI: 10.1021/acs.joc.6b02295
J. Org. Chem. 2016, 81, 11819−11830

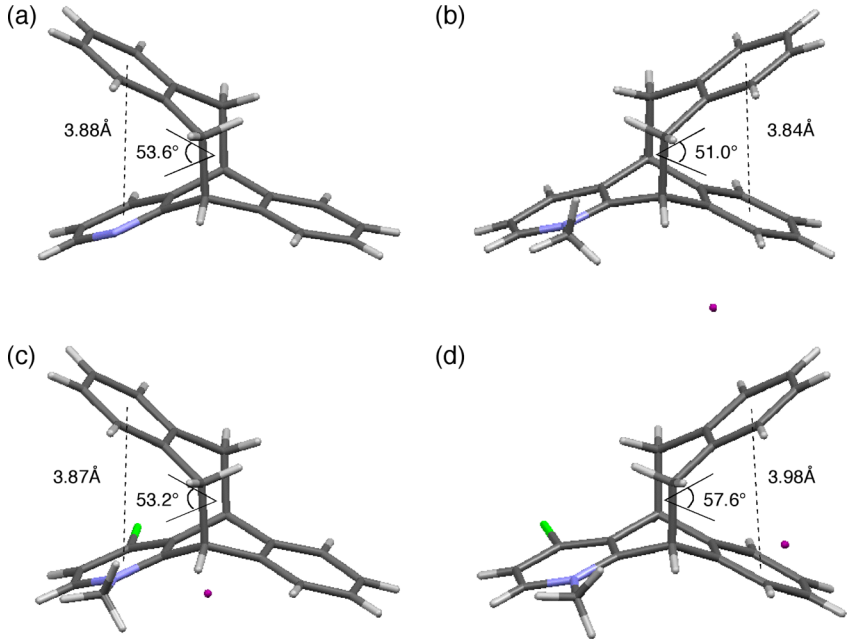

Figure 3. X-ray structures of (a) **1** and (c) **2**·MeI(A) with conformation **A**, and (b) **1**·MeI and (d) **2**·MeI(B) with conformation **B**.

The quarternization of the pyridine ring of **1**-**3** and **5** with methyl iodide gave the corresponding *N*-methylpyridinium iodide **1**·MeI, **2**·MeI, **3**·MeI and **5**·MeI in 77−93% yields, and the methylation of **1** with methyl bromide gave **1**·MeBr in 79% yield. The bromide ion of **1**·MeBr was replaced with the other anions to produce various salts with a different counteranion.

X-ray Structures. The structures of these balances, except for **5**·MeI, were confirmed by X-ray structural analysis. Figure 3 shows the X-ray structures of **1**, **1**·MeI and **2**·MeI. The structure of **1** adopted the geometry of conformer **A**, with the benzene ring of the mobile unit close to the benzene ring of the base unit with a distance of 3.88 Å between the centroids. Contrary to our expectations, the structures of **1**·MeI adopted the geometry of conformer **B**, with the benzene ring of the mobile unit close to the benzene ring of the base unit with a distance of 3.84 Å between the centroids. However, intermolecular cation−π interactions were observed between the pyridinium and benzene rings. The molecules form a columnar motif that is stabilized by $Py^+\cdots Ar$ interactions with a distance of 3.673 Å (Figure S5). This may be due to the formation of more stable crystals through intermolecular cation−π interactions.

The X-ray structure of **2**·MeI shows two independent molecules **2**·MeI(A) and **2**·MeI(B) in an asymmetric unit. These two molecules adopted conformers **A** and **B**, which are shown in Figure 3c and 3d, respectively. A comparison of these two structures clarified the effect of cation−π and π−π interactions on the geometries of **A** and **B**. The distance between the centroids for **2**·MeI(A) and **2**·MeI(B) are 3.87 and 3.98 Å, respectively. In addition, the 53.2° of interplanar angle for **2**·MeI(A) was smaller than that of **2**·MeI(B) (57.6°). These geometrical differences are thought to be due to the difference in strength between the cation−π and π−π interactions.

Shimizu has reported that the energy of the pyridinium−π interaction depends on the stacking mode of the *N*-methylpyridine with the benzene ring, with a proximal geometry being more stable than a distal geometry.[24] This is explained by the contribution of the CH···π interaction between the methyl group and the benzene ring. In our balances, the two rings are displaced with interplanar angles of ca. 50 degrees and the *N*-methyl group is set apart from the benzene ring due to the rigid framework structure. In the case of **2**·MeI, the distance between the hydrogen atom of the methyl moiety and the carbon atom of the benzene ring is 3.57 Å, which is much longer than common cutoff distance (3.05 Å) for a CH−π interaction.

Optimized Structures. Structure optimization for conformers of **A** and **B** of **1**, **1**·Me^+, **2**·Me^+, **3**·Me^+, **4** and **5**·Me^+ were carried out by MP2 calculations at the 6-311G* level, and the energies and ΔE values ($E_{confA} - E_{confB}$) are listed in Table 1. A comparison of the energies between conformers **A** and **B** revealed that conformers **A** are more stable than conformers **B** by −2.11 to −4.23 kcal/mol. The reported interaction energy between *N*-methylpyridinium and benzene rings is −7.88 kcal/mol for a slipped-parallel dimer, whereas that of a benzene dimer is −2.48 kcal/mol,[7] so that the estimated ΔE value should be −5.40 kcal/mol. This difference in the ΔE values is attributable to the differences between the restricted and the ideal geometries. The calculated interplanar angles of the two rings (θ value) are around 40−50°. These larger θ values are due to the rigid framework structure of the molecular balance and the restricted motion of the aromatic ring in the mobile unit. It is well-known that the parallel stacking of aromatic rings gives rise to repulsive forces between them.[33] The larger interplanar angle in these balances would reduce the repulsive force. The θ values of conformers **A** are smaller than those of conformers **B**. In addition, the distances between the two centroids (d value) of conformers **A** are shorter than those of conformer **B**. These results are in agreement with those observed in the X-ray structures of **2**·MeI described above. The relatively larger θ values and longer d values observed in the X-ray structures are thought to be the results of packing effects.

Determination of ΔG Values. We first attempted to use dynamic ^{1}H NMR spectroscopy in CD_2Cl_2 to assess the population of conformers **A** and **B** shown in Figure 1. Although the methylene protons coalesced at 181 K,[21] the two conformers

DOI: 10.1021/acs.joc.6b02295
J. Org. Chem. 2016, 81, 11819−11830

Table 1. Φ_A and ϕ_B Values Obtained from the Optimized Geometries and the X-ray Structures, and the Calculated Boundary J_A and J_B Values

compd	source	conf.	E (kcal/mol)[a]	ΔE (kcal/mol)[b]	Φ_A (deg)	Φ_B (deg)	J_A (Hz)	J_B (Hz)
1	X-ray	A			6.63	–[c]	10.43	–[c]
1	Calculation	A	−541370.10	−0.51	4.69		10.44	
1		B	−541369.59			106.27		2.07
1·MeI	X-ray	B			–[d]	109.55	–[d]	2.49
1·Me$^+$	Calculation	A	−566194.42	−3.05	4.35		10.45	
		B	−566191.37			110.27		2.59
2·MeI	X-ray	A			5.59		10.41	
2·MeI	X-ray	B				107.83		2.26
2·Me$^+$	Calculation	A	−854260.79	−4.01	3.76		10.45	
		B	−854256.78			110.88		2.74
3·MeI	X-ray	B				112.12		2.85
3·Me$^+$	Calculation	A	−650012.44	−3.35	1.49		10.51	
		B	−650009.09			103.68		1.83
4	X-ray	A			8.17[e]		10.15[e]	
4	Calculation	A	−588443.74	−2.11	4.21[e]		10.32[e]	
		B	−588441.63			112.13[f]		2.93[f]
5·Me$^+$	Calculation	A	−709564.94	−4.23	–	–		
		B	−709560.71		4.88		10.42	

[a]Calculated by MP2/6-311G* level. [b]ΔE values indicate the values of ($E_{confA} - E_{confB}$). [c]The X-ray structure for conformer **B** could not be obtained. [d]The X-ray structure for conformer **A** could not be obtained. [e]$\Phi_{A(H4,H5)}$ value was used for the calculation of the J value. [f]$\Phi_{B(H4,H5)}$ value was used for the calculation of the J value.

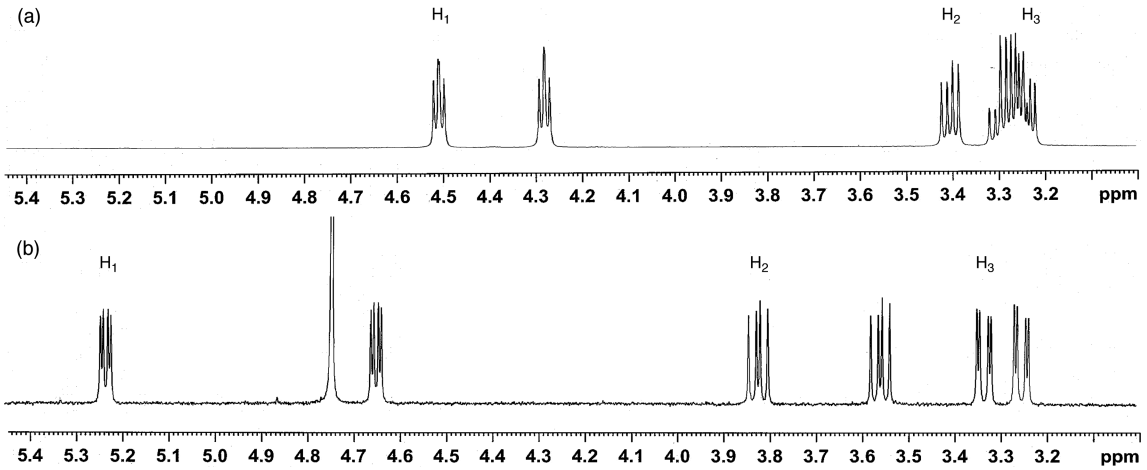

Figure 4. ^{1}H NMR spectra at 600 MHz for the methine and methylene protons of (a) **1** and (b) **1**·MeI in $CDCl_3$.

were not separated at temperatures above the freezing point of this solvent, suggesting that the interconversion energy is much smaller than that required to separate the two conformers. Fukazawa et al. reported that the activation energy of a similar system is estimated to be 7 kcal/mol, and the conformers were not separated in ^{1}H NMR at lower temperatures.[34] Therefore, we examined an alternative approach on the basis of the changes in the coupling constants of a bridgehead methine proton, which was successfully used to estimate ΔG values of related seesaw balances by Motherwell and Aliev.[20] Figure 4 shows the ^{1}H NMR spectra for the methine and methylene protons of **1** and **1**·MeI in $CDCl_3$. The methine proton H_1 of **1** appeared at δ 4.51, which coupled differently to vicinal protons H_2 and H_3 to show a doublet of doublets with coupling constants of 7.66 and 6.02 Hz, respectively. On the other hand, in the case of **1**·MeI, H_1 appeared at δ 5.23 with coupling constants of 9.83 and 3.95 Hz for $J_{H1,H2}$ and $J_{H1,H3}$, respectively. The differences in the $J_{H1,H2}$ values between **1** and **1**·MeI can be explained by changes in the population of conformers **A** and **B** arising from the quarternization of the pyridine ring. These observed averaged coupling constants are a function of the population of the conformers, N_A and N_B, and can be defined by the following eq 1, where J_A and J_B are the boundary values of the corresponding coupling constants for conformers **A** and **B**, respectively.

$$J_{obs} = N_A J_A + N_B J_B \quad (1)$$

The boundary J_A and J_B values of the corresponding conformers **A** and **B** can be obtained from the H_1−C−C−H_2 torsion angles, $\phi_{A(H1,H2)}$ and $\phi_{B(H1,H2)}$. The J values are defined by the Karplus−Altona eq 2,[35] where P_1−P_6 are empirically determined parameters, $\Sigma\Delta\chi_i$ is the sum of the electronegative differences between the substituent attached to the ethane fragment and hydrogen, and ξ_I stands for +1 or −1 according to the orientation of the substituent.

$$J(\phi) = P_1 \cos^2 \phi + P_2 \cos \phi + P_3 + \Sigma\Delta\chi_i\{P_4 + P_5 \cos^2(\xi_i \cdot \phi + P_6 \cdot |\Delta\chi_i|)\} \quad (2)$$

DOI: 10.1021/acs.joc.6b02295
J. Org. Chem. 2016, 81, 11819−11830

The values for $\phi_{A(H1,H2)}$ and $\phi_{B(H1,H2)}$ were determined from the optimized geometries and X-ray structures, which are listed in Table 1. In most cases, there was little difference between the experimental and calculated ϕ values, except for the $\phi_{B(H1,H2)}$ value of **3**·MeI. This is attributable to the difference in the geometries around the Me_2N moiety; the Me_2N group in the X-ray structure is twisted in the opposite direction to that in the optimized geometry. In the optimized geometry of balance **4**, as intramolecular N−O···H bonding was observed, the $\phi_{A(H4,H5)}$ and $\phi_{B(H4,H5)}$ values were used for the determination of the J values. Table 1 lists the boundary J_A and J_B values obtained on the basis of the values of the dihedral angles ϕ_A and ϕ_B using the Karplus-Altona eq 2. As the J values originating from the X-ray structures are very close to those obtained from the calculations, it seems reasonable to use the calculated boundary J_A and J_B values for the quantification of the interaction energies. A comparison of J_{obs} with the J_A and J_B values led to the N_A and N_B using eq 1. On the basis of these populations, ΔG values were obtained using eq 3.

$$\Delta G = -RT \ln(N_A/N_B) \quad (3)$$

For balance **1**, the ratio of conformer **A** to **B** is 66.4:33.6, leading to −0.4 kcal/mol of ΔG in $CDCl_3$. Similarly, −1.47 kcal/mol of ΔG was obtained for **1**·MeI. The preference for conformer **A** rather than conformer **B** in solution was confirmed by NOESY measurement, where a correlation was observed between *N*-CH_3 and the aromatic proton of the mobile unit, and no correlation was observed between the two aromatic ring protons.[23] The calculated ΔG values listed in Table 1 support the preference for conformer **A**.

Solvent and Substituent Effects. Table 2 shows the J_{obs}, N_A, N_B and ΔG values for **1**·MeI. The ΔG values were in the range of −0.47 to −1.47 kcal/mol. This clearly shows that the solvents have a significant effect on the conformer ratio of **1**·MeI. Dougherty and co-workers[36] reported a solvent effect on the cation−π interaction between methylammonium and benzene based on computational studies, where a linear relationship was observed between ΔG and $1/\varepsilon$. A similar trend was observed in the present case shown in Figure 5; a good linear relationship was observed between ΔG and $1/\varepsilon$ with the exclusion of the ΔG value in CD_3OD. As it has been shown that the association energy for ion-pairs is correlated with $1/\varepsilon$,[37] the cation−π interaction surpasses the steric and electrostatic disadvantages associated with ion-pair formation. The reason for the larger ΔG value in CD_3OD may be a result of the H-bond between the solvent with an anion, which is supported by the larger $-T\Delta S$ value as described below. A similar tendency was also observed for the other balances (Table 3). The relatively lower ΔG value in CD_3CN is thought to be due to an interaction between the iodide ion and CH_3CN.[38] The effect of solvent polarity described above can be explained by the interaction of solvents with the pyridinium surfaces, which weakens the interaction between the pyridinium and benzene rings. This solvent effect is parallel with that for the *N*-methylated proximal balance reported by Shimizu.[24]

Table 2. ΔG Values for 1·MeI Obtained from J Values in Various Solvents[a]

solv	J_{obs} (Hz)[b]	N_A (%)	N_B (%)	ΔG (kcal/mol)[c]	ε	$1/\varepsilon$
$CDCl_3$	9.83	91.7	0.83	−1.47	4.8	0.208
CD_2Cl_2	9.40	86.2	13.8	−1.11	8.9	0.112
$(CD_3)_2CO$	8.66	76.9	23.1	−0.73	20.6	0.049
CD_3OD	9.22	84.04	16.0	−1.01	32.7	0.031
CD_3CN	8.00	68.5	31.5	−0.47	35.9	0.028
$(CD_3)_2SO$	8.24	71.5	28.5	−0.55	46.4	0.022

[a]A 1.0 mM solution was used for the measurement of ^{1}H NMR at 298 K. [b]Determined by ^{1}H NMR. The coupling constants were measured within an error range of ±0.01 Hz using the expanded spectra. [c]The error in the ΔG values is estimated to be within ±0.01 kcal/mol.

Similar to the case of **1**·MeI, the ΔG values for **2**·MeI and **3**·MeI show a good correlation with $1/\varepsilon$ on exclusion of the ΔG values in CD_3OD, as shown in Figure 5. The slope of these plots differ significantly from each other. The slope observed for **2**·MeI is steeper than that for **3**·MeI, showing that the effect of the solvent on **2**·MeI is larger than that on **3**·MeI. This is thought to be due to the enhancement of the positive charge in the pyridinium ring by a chlorine substituent, resulting in a stronger attractive force. On the other hand, the Me_2N group serves as an electron-donating group, leading to a weakening of the cationic charge in the pyridinium ring. As electrostatic interaction is a major force in the cation−π interaction,[1,7] these substituent effects can be explained by differences in the charge density of the pyridinium ring. The H-bond of the balances with CD_3OD is thought to be one reason for their failure to fit the linear relationship as observed in the case of **1**·MeI. Figure 6 shows plots of the ΔG values for **4** and **5**·MeI. In these cases, rough linear correlations were observed. The slopes are much gentler than those of the other plots shown in Figure 5, indicating a smaller solvent dependence of the ΔG values.

It should be noted that although the balance **4** is a neutral compound, we still observed an attractive interaction between the pyridine *N*-oxide and the benzene ring. These two slopes are almost in parallel, but the ΔG values for **5**·MeI are much larger than those of **4**. This is in agreement with the calculated ΔE values, with that for **5**·MeI being much larger than that of **4**. Although the methoxy group was expected to enhance the interaction with the pyridinium ring, it was not effective in nonpolar solvents. It was, however, effective in polar solvents in comparison to **1**·MeI.

Figure 7 provides a summary of substituent dependence on the ΔG values in various solvents. It is clear that **2**·MeI, having a chlorine substituent, is the most significantly affected by the solvent among these balances. On the other hand, **5**·MeI, having two methoxy substituents at the aromatic ring, is affected only slightly by the solvent, resulting in the ΔG values being the largest among these balances in polar solvents. The ΔG values of all balances are close together in CD_3OD, indicating that the CD_3OD canceled out the substituent effect.

Due to the difficulty of dissecting the electronic and steric effects of the substituent, there has been only one experimental report on the effect of substituents on cation−π interactions. Hunter and co-workers reported the effect of the substituent at the aromatic ring on the edge-to-face pyridinium−π interaction using double-mutant cycles.[39] Introduction of a Me_2N group to the benzene ring led to an increase in the interaction energy from −0.6 kcal/mol to −1.87 kcal/mol. The effect of this electron-donating group is comparable to that of the calculated ΔE value (−4.23 kcal/mol) for **5**·MeI, having two methoxy groups at the benzene ring, which is the highest value among the seesaw balances discussed herein (Table 1).

To elucidate the contribution of the substituent on the cation−π interaction, electrostatic potentials were calculated for each balance as electrostatic interaction is a major force of a cation−π interaction. Figure 8 illustrates electrostatic potential

DOI: 10.1021/acs.joc.6b02295
J. Org. Chem. 2016, 81, 11819−11830

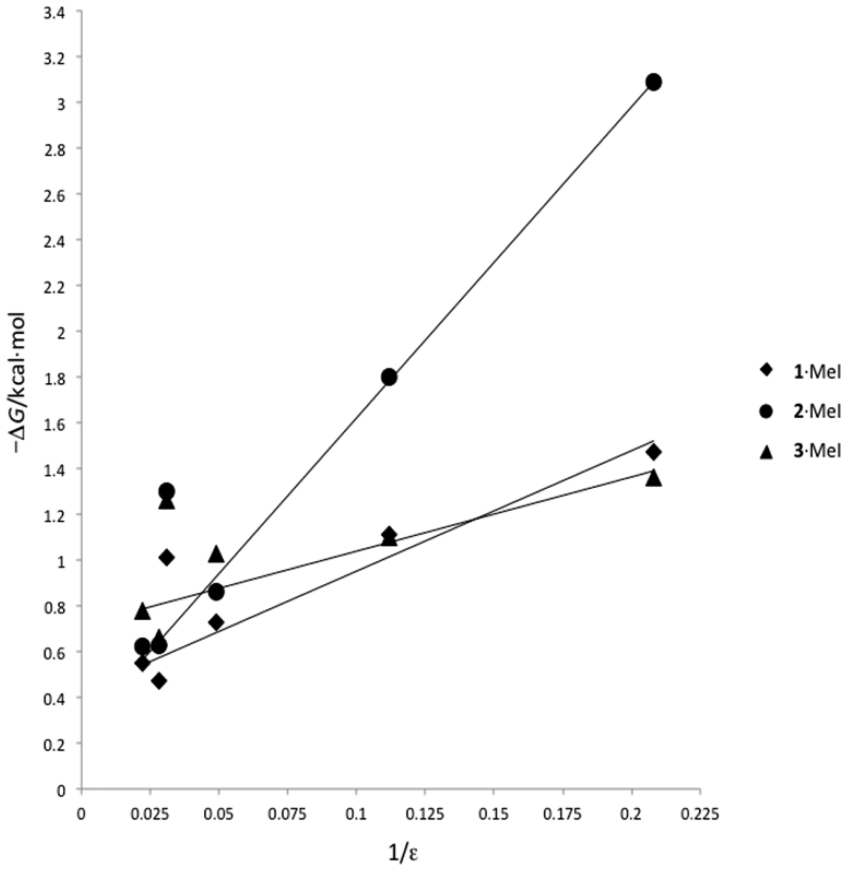

Figure 5. Plots of ΔG vs $1/\varepsilon$ for **1**·MeI (r^2 = 0.965 after exclusion of the ΔG value in CD_3OD), **2**·MeI (r^2 = 0.998 after exclusion of the ΔG value in CD_3OD) and **3**·MeI.

Table 3. ΔG Values for 1, 1·MeI, 2·MeI, 3·MeI, 4 and 5·MeI in Various Solvents[a,b]

	ΔG (kcal/mol)[c]					
solv	**1**	**1**·MeI	**2**·MeI	**3**·MeI	**4**	**5**·MeI
$CDCl_3$	−0.41	−1.47	−3.09	−1.36	−0.85	−1.33
CD_2Cl_2	−0.17	−1.11	−1.8	−1.1	−0.65	−1.32
$(CD_3)_2CO$	−0.17	−0.73	−0.86	−1.03	−0.76	−1.36
CD_3OD	−0.57	−1.01	−1.3	−1.26	−1.1	−1.25
CD_3CN	−0.16	−0.47	−0.63	−0.66	−0.53	−1.12
$(CD_3)_2SO$	−0.16	−0.55	−0.62	−0.78	−0.64	−1.14

[a]A 1.0 mM solution was used for the measurement of ^1H NMR at 298 K. [b]Determined by ^1H NMR. The coupling constants were measured within an error range of ±0.01 Hz using the expanded spectra, which are shown in Supporting Information. [c]The error in the ΔG values is estimated to be within ±0.01 kcal/mol.

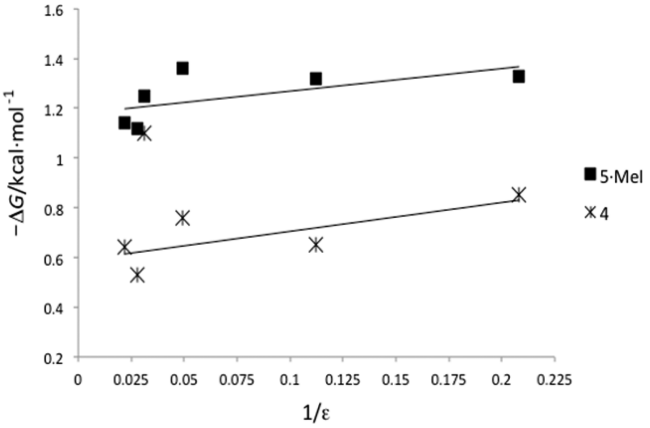

Figure 6. Plots of ΔG vs $1/\varepsilon$ for **4** and **5**·MeI.

maps for both conformers **A** and **B** of the molecular balances projecting from the side of the pyridinium and benzene rings to clarify the differences in the electrostatic potentials between conformers **A** and **B**. Comparison of the electrostatic potentials between conformers **A** and **B** of each balance clearly shows considerable differences in the potentials of the pyridinium and benzene rings depending on the substituent. With respect to the pyridine rings, the potentials of conformers **A** were more negative than those of **B**, showing the obvious attractive electrostatic interactions in each molecule. In particular, the difference in balance **5**·Me^+ was more intense, predicting a stronger electrostatic interaction. However, the electrostatic interaction is not reflected in the observed ΔG values of **5**·Me^+ in nonpolar solvents; therefore, contribution of another factor such as a steric repulsion is likely to be important in this system. In the case of neutral balance **4**, an electrostatic interaction was still observed in conformer **A**; the potential of **4**-**A** was more negative than that in **4**-**B**. This shows that an attractive interaction was observed between the pyridine *N*-oxide and the benzene ring due to the charge separated structure of the N^+-O^- moiety. On the other hand, with respect to the benzene rings, the electrostatic potential of conformer **A** depended on the substituents. The potential in **2**·Me^+ was less negative than that of **1**·Me^+, and the potential in **3**·Me^+ was more negative than **1**·Me^+, clearly showing the inductive effect of the substituent on the interaction strength. This tendency is in parallel

DOI: 10.1021/acs.joc.6b02295
J. Org. Chem. 2016, 81, 11819−11830

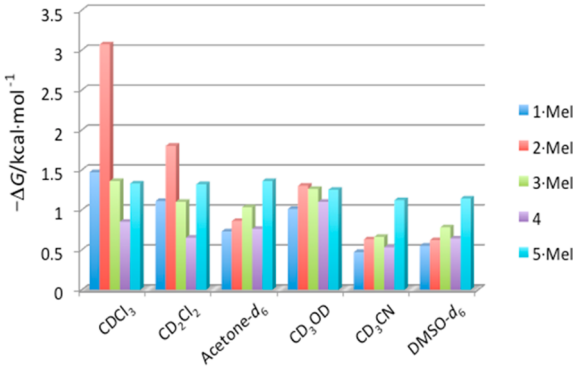

Figure 7. Substituent dependence on the ΔG values in various solvents.

with the order of ΔG values shown in Table 3 (**2**·MeI > **1**·MeI > **3**·MeI).

Counteranion Effect. Next, the counteranion effect on the ΔG values was investigated. The counteranion effect depends on the ion pair and aromatic systems. It has been reported that in the complexation of cations with cyclophane receptors, the association constant is correlated to the cation−anion attraction of the ion-pair.[40] Hunter and colleagues applied chemical double mutant cycles to three-component systems, and confirmed that the intermolecular $Py^+\cdots Ar$ interaction energy is independent of the counteranions.[41] On the other hand, as the effect on the intramolecular interaction has not yet been evaluated, we presumed that our system could be used to evaluate the counteranion effect on intramolecular cation−π interactions.

To clarify the counteranion effect on the intramolecular $Py^+\cdots Ar$ interactions, the ΔG values of **1**·MeX possessing various counteranions were measured in $CDCl_3$ and $(CD_3)_2CO$. Table 4 shows the ΔG values for **1**·MeX and the ion radii r_{ci}[42] as we thought that the ion size would affect the intramolecular interactions. The ΔG values in $CDCl_3$ were in the range of −1.19 to −2.04 kcal/mol, suggesting that the counteranion had

Table 4. ΔG Values for 1·MeX with a Variety of Anions in $CDCl_3$ and $(CD_3)_2CO$, and Ionic Radii

Anion	r_{ci} (pm)	$\Delta G_{(CD3)2CO}$[b] (kcal/mol)	ΔG_{CDCl3}[a] (kcal/mol)
Cl^-	181	−2.04	−0.76
Br^-	196	−1.78	−0.75
I^-	220	−1.47	−0.73
BF_4^-	228	−1.41	−0.75
CH_3COO^-	232	−1.19	−0.72
PF_6^-	245	−1.21	−0.75

[a]A 1.0 mM solution was used for the measurement of ^1H NMR at 298 K in $CDCl_3$. [b]A 1.0 mM solution was used for the measurement of ^1H NMR at 298 K in $(CD_3)_2CO$.

a significant effect on the ΔG. Figure 9 shows plots of ΔG vs r_{ci}. A good linear correlation was observed between them after the exclusion of an acetate ion, with the ΔG decreasing as the ion size increased. A hydrogen bond between the acetate ion and a pyridinium proton may explain its failure to fit the linear relationship, which is supported by ^1H NMR chemical shifts; the δ H2 values for the pyridinium ring of **1**·MeOAc and **1**·$MePF_6$ appear at δ 10.01 and 8.37, respectively, indicating a stronger H-bond between the acetate ion and the H2.[43] In $(CD_3)_2CO$, unlike $CDCl_3$, ion size had little effect on the ΔG value. These results can be explained by the fact that the anion binds with a cation to form an ion-pair in nonpolar solvents (Figures 10a and 10b) and, therefore, the steric bulkiness of the counteranion hinders intramolecular attraction. On the contrary, in polar solvents, both the cation and the counteranion are solvated and they are separated from each other (Figures 10c and 10d), as a result, the ΔG values are independent of the counteranions. Although a polar solvent abolished the counteranion effect, it simultaneously disturbed the cation−π interaction, leading to a smaller ΔG value.

Thermodynamic Parameters. To gain further insights into the details of the solvent, counteranion and substituent effects on the ΔG values, the thermodynamic parameters were

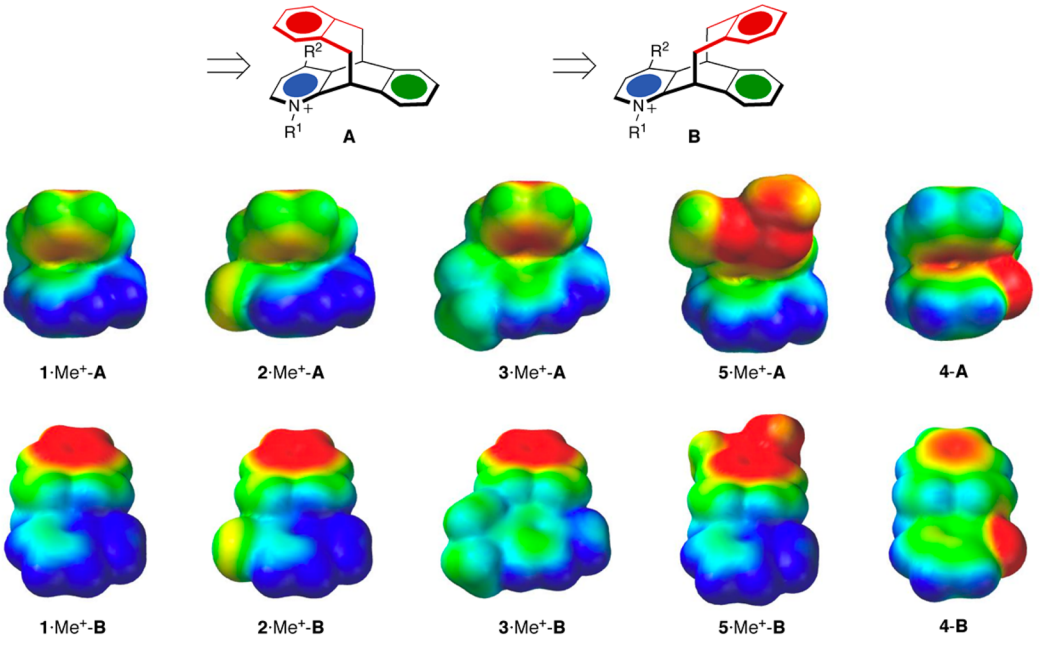

Figure 8. Electrostatic potential maps of conformers **A** and **B** for molecular balances **1**·Me^+, **2**·Me^+, **3**·Me^+, **4** and **5**·Me^+. Colors correspond to 200 kJ/mol (blue) to 400 kJ/mol (red) for **1**·Me^+, **2**·Me^+, **3**·Me^+ and **5**·Me^+, and −100 kJ/mol (blue) to 100 kJ/mol (red) for **4**.

DOI: 10.1021/acs.joc.6b02295
J. Org. Chem. 2016, 81, 11819−11830

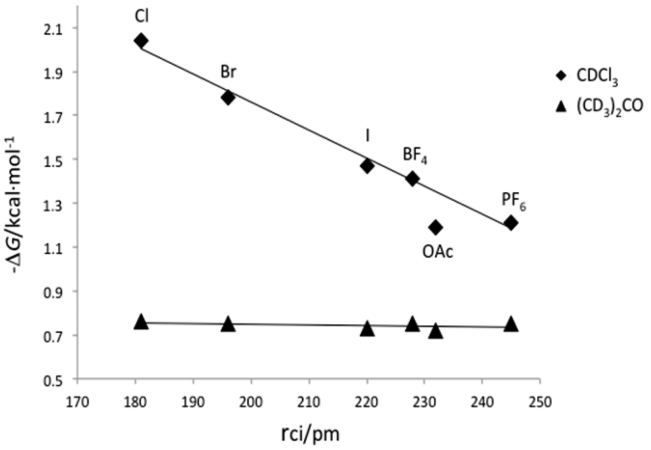

Figure 9. Plots of ΔG vs r_{ci} for **1**·MeX in $CDCl_3$ (r^2 = 0.991 after exclusion of the ΔG value for an acetate ion) and in $(CD_3)_2CO$.

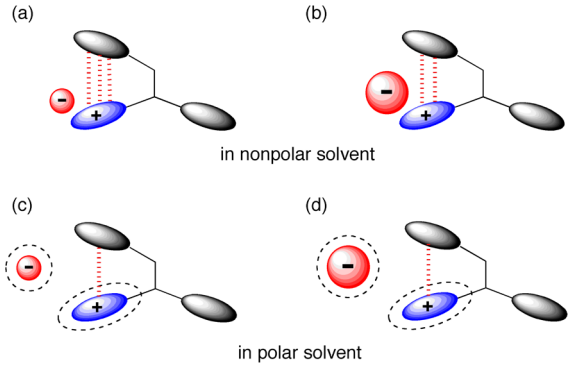

Figure 10. Schematic representation of **1**·MeX with (a) smaller and (b) larger counteranions in a nonpolar solvent, and **1**·MeX with (c) smaller and (d) larger counteranions in a polar solvent, the dotted lines of which show the solvation by a polar solvent.

obtained for molecular balances **1**·MeI, **1**·MeCl, **2**·MeI, **3**·MeI, **4** and **5**·MeI in $CDCl_3$, $(CD_3)_2CO$ and CD_3OD by the van't Hoff plot using eq 4 at the temperature range of 281−325 K.

$$\ln (N_A/N_B) = -\Delta H/RT + \Delta S/R \quad (4)$$

Figure 11 shows plots of $\ln(N_A/N_B)$ vs $1/T$ for **1**·MeI and **1**·MeCl in $CDCl_3$, $(CD_3)_2CO$ and CD_3OD. Good linear correlations were observed for each. The $\ln(N_A/N_B)$ values of **1**·MeCl at 281 K could not be obtained as the J_{obs} value was almost the same as the boundary J values. The slope is significantly dependent on the property of the solvent; the slopes observed in $(CD_3)_2CO$ and CD_3OD were much gentler than that in $CDCl_3$. The $\Delta H°$ and $-T\Delta S°$ values obtained from the plots are shown in Table 5. The data show that all enthalpies are negative. The absolute $\Delta H°$ values for **1**·MeI, **1**·MeCl, **2**·MeI and **3**·MeI in $CDCl_3$ are much larger than those in $(CD_3)_2CO$ and CD_3OD. The $T\Delta S°$ values in $CDCl_3$ are negative, but the values in the polar solvents are positive. These findings suggest that the contribution of solvation to the ΔG values is significant in $(CD_3)_2CO$ and CD_3OD. The larger negative $\Delta H°$ value for **1**·MeCl than for **1**·MeI supports the notion of a counteranion effect in which a smaller chloride ion exerts less steric hindrance than an iodide ion on the intramolecular attraction. The larger negative entropy indicates stronger ion pair formation between the cation and a chloride ion as well as a H-bond between them.

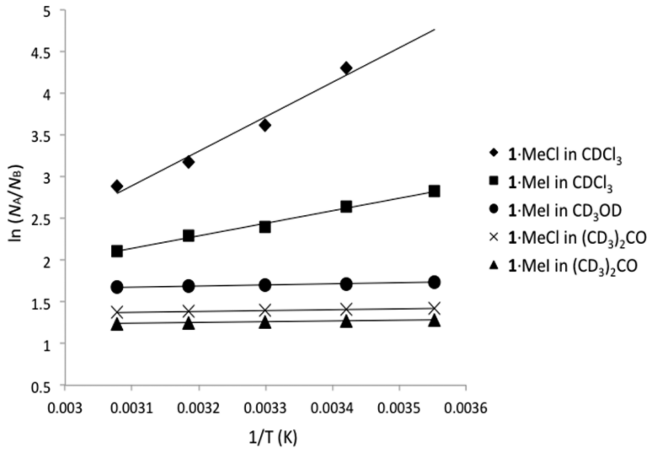

Figure 11. Van't Hoff plots for **1**·MeCl in $CDCl_3$ and $(CD_3)_2CO$, and **1**·MeI in $CDCl_3$, CD_3OD and $(CD_3)_2CO$.

Table 5. $\Delta H°$ and $\Delta S°$ Values for 1·MeI, 1·MeCl, 2·MeI, 3·MeI, 4 and 5·MeI Obtained from Van't Hoff Plots[a,b]

compd	solv	$\Delta H°$ (kcal/mol)	$-T\Delta S°$ (kcal/mol)
1·MeI	$CDCl_3$	−3.02 ± 0.04	1.514 ± 0.01
	$(CD_3)_2CO$	−0.20 ± 0.03	−0.551 ± 0.02
	CD_3OD	−0.25 ± 0.01	−0.766 ± 0.01
1·MeCl	$CDCl_3$	−6.59 ± 0.17	4.36 ± 0.2
	$(CD_3)_2CO$	−0.22 ± 0.01	−0.60 ± 0.01
2·MeI	$CDCl_3$	–[c]	–[c]
	$(CD_3)_2CO$	−0.19 ± 0.01	−0.67 ± 0.01
	CD_3OD	−0.29 ± 0.01	−1.01 ± 0.04
3·MeI	$CDCl_3$	−2.12 ± 0.003	0.79 ± 0.01
	$(CD_3)_2CO$	−0.75 ± 0.05	−0.304 ± 0.01
	CD_3OD	–[d]	–[d]
4	$CDCl_3$	−0.73 ± 0.04	0.125 ± 0.01
	$(CD_3)_2CO$	−0.80 ± 0.14	0.057 ± 0.01
	CD_3OD	−1.65 ± 0.01	0.349 ± 0.01
5·MeI	$CDCl_3$	−1.36 ± 0.02	0.039 ± 0.02
	$(CD_3)_2CO$	−2.11 ± 0.02	0.71 ± 0.02
	CD_3OD	−1.44 ± 0.03	0.164 ± 0.04

[a]A 1.0 mM solution was used for the measurement of ^{1}H NMR. [b]Details of the calculations of $\Delta H°$ and $\Delta S°$ are shown in Tables S12−S41 and Figures S19−S33. [c]The J_{obs} values exceeded the boundary J value. [d]The J value could not be measured as the solvent peak overlapped with the methine peak.

As compound **4** has no counteranion, the $-T\Delta S°$ values were positive due to weak solvation, leading to a smaller solvent effect on ΔG values. However, the relatively larger $\Delta S°$ and absolute $\Delta H°$ values observed in CD_3OD suggested that the *N*-oxide moiety ($-N^+-O^-$) forms a H-bond with CD_3OD, which is thought to promote charge separation and enhance intramolecular cation−π interaction. In the case of balance **5**, the $\Delta H°$ values in polar solvents are considerably more negative than those of the other *N*-methyl salts, suggesting stronger attractive forces between the pyridinium and the electron-rich aryl group. Although the reason for the smaller absolute $\Delta H°$ values in nonpolar solvents than those of the other *N*-methyl balances is not clear, this may be attributable to some degree on the steric effect with respect to the two methoxy groups of the aromatic ring.

CONCLUSION

We developed a series of new seesaw balances having two distinct conformers, **A** and **B**, which are stabilized by pyridinium−π and

DOI: 10.1021/acs.joc.6b02295
J. Org. Chem. 2016, 81, 11819−11830

$\pi-\pi$ interactions, respectively. These molecular balances with a restricted motion were effective in allowing the investigation of the solvent and counteranion, as well as substituent, effects on pyridinium$-\pi$ interactions. The quantification of the ΔG values for these molecular balances revealed that polar solvents hinder the cation$-\pi$ interaction by solvation of the cation and anion. The counteranion effect in the intramolecular cation$-\pi$ system was also clarified for the first time. The size of the counteranion had a significant effect on the ΔG values of the molecular balances. The formation of an ion-pair with a larger counteranion in the nonpolar solvents reduces the ΔG values due to steric hindrance to the intramolecular attraction. On the other hand, in polar solvents, the ΔG values were independent of the counteranions. In addition, the substituent effects were systematically investigated. The substituent at the pyridine ring had a large effect on the ΔG value of the cation$-\pi$ interaction. While an electron-withdrawing chlorine substituent enhanced the interaction, an electron-donating dimethylamino substituent weakened the interaction. These results were in agreement with those obtained by comparison of electrostatic potentials between conformers **A** and **B**. One remarkable feature is that in the pyridine *N*-oxide **4**, which is a neutral molecule, a pyridinium$-\pi$ interaction forms between the pyridinium moiety and the benzene ring. The highest ΔG value was observed in CD_3OD, highlighting that this balance shows significantly different behavior from the other balances. Thermodynamic parameters obtained by van't Hoff plots furthered our understanding of these observations.

The establishment of the synthesis and evaluation of this type of seesaw balances will enable the further development of various molecular balances. In addition, their applications to molecular switches, sensing materials and catalysts are expected due to the higher interaction energy of the cation$-\pi$ interactions in comparison with other π-interactions.

EXPERIMENTAL SECTION

General Information. Unless otherwise noted, reagents and starting materials were purchased from traditional suppliers and were used without further purification. Column chromatography was carried out using silica gel 60 N. TLC was carried out on silica gel 60 PF_{254}. IR spectra were recorded as neat films between NaCl plates or KBr pellets. ^{1}H NMR spectra were obtained at 600 MHz as dilute solution in $CDCl_3$, CD_2Cl_2, acetone-d_6, CD_3OD, CD_3CN, and DMSO-d_6. The chemical shifts were reported relative to internal TMS. ^{13}C NMR spectra were obtained at 100 or 150 MHz as dilute solution in $CDCl_3$, and the chemical shifts were reported relative to internal TMS. The NMR coupling constants were determined by using expanded spectra. The measurement of the distances between the coupled peaks with a scale gave the *J* values within the error of ±0.02 Hz. High- and low-resolution mass spectra were recorded on Orbitrap LC−MS using ESI ionization mode. X-ray measurements at 123 K were carried out using an imaging plate area detector with graphite monochromated Cu−Kα radiation. All calculations were performed using the CrystalStructure crystallographic software package except for refinement, which was performed using SHELXL-97 or SHELXL-2013. The raw data frames were integrated with the SAINT+ program by using a narrow-frame integration algorithm. All structures were solved by a combination of direct methods and difference Fourier syntheses, and refined by full-matrix least-squares on F^2, by using the SHELXTL software package. Microwave irradiations were conducted using a Biotage Initiator+ (0−400W), equipped with external IR-sensor temperature monitoring from the side of the vessel and stirring unit in the bottom of the vessel.

Synthesis of Compound ***1***. To a solution of azaanthracene[23,25a] (457.5 mg, 2.55 mmol) in 4 mL of diethyl phthalate[28a,b] was added 1,3-dihydrobenzo[*c*]thiophene-2,2-dioxide[26a] (473.1 mg, 2.82 mmol) at 270 °C using a dry block bath with stirrer and the solution was stirred for 3 h. The diethyl phthalate was hydrolyzed with 20 mL of 8% sodium hydroxide solution at 90 °C for 15 h under stirring. After the solution was cooled to room temperature, the precipitates were collected by filtration, and the filtrate was extracted with 100 mL of benzene. The benzene layer was worked up in the usual manner to give a crude oil. This oily product and the filtered solid were subjected together to silica gel chromatography with a 2:1 mixture of hexane-ethyl acetate as an eluent to give a crude solid, which was purified by GPC with chloroform yielded **1** as a colorless solid (143.3 mg, 21.6%). This was recrystallized from $CH_2Cl_2-CH_3CN$ gave colorless crystals suitable for X-ray structural analysis; mp 196.3−197.2 °C; IR (KBr) 3032, 2995, 2930, 1624, 1505, 1490, 1455, 780, 768, 752, 652, 598, 576 cm^{-1}; ^{1}H NMR (600 MHz, $CDCl_3$) δ 8.22 (dd, *J* = 1.8, 4.8 Hz, 1H), 7.40 (dd, *J* = 1.8, 7.8 Hz, 1H), 7.21−7.26 (m, 2H), 7.09−7.13 (m, 2H), 6.94 (dd, *J* = 4.8, 7.5, 1H), 6.82−6.92 (m, 3H), 4.51 (dd, *J* = 6.0, 7.7 Hz, 1H), 4.28 (dd, *J* = 6.0, 7.6 Hz, 1H), 3.40 (dd, *J* = 7.8, 15.0 Hz, 1H), 3.22−3.32 (m, 3H); ^{13}C NMR ($CDCl_3$, 150 MHz); δ 162.8, 146.4, 142.3, 142.1, 139.7, 139.5, 137.0, 134.0, 130.5, 130.1, 127.2, 126.4, 126.4, 126.3, 126.3, 126.2, 121.0, 48.2, 44.6, 44.3, 43.3; MS (ESI) *m*/*z* 284 (M^+ + 1, 100); HRMS calcd for $C_{21}H_{17}N$ $[M + 1]^+$ 284.1439, found for 284.1448.

Microwave Synthesis of Compound ***1***. To a 5 mL microwave vial was added azaanthracene **6** (178 mg, 0.992 mmol) and 1,3-dihydrobenzo[*c*]thiophene-2,2-dioxide **7** (249 mg, 1.49 mmol). Subsequently, toluene (2.5 mL) was added to the vial. The reaction vial was then sealed and the mixture was heated at 280 °C for 4.5 h under stirring utilizing microwave irradiation. The reaction mixture was cooled to room temperature, and removal of the solvent left a crude oil. This oily product was subjected to silica gel chromatography with a 1:1 mixture of hexane-ethyl acetate as an eluent to give a crude solid, which was purified by GPC with chloroform yielded **1** as a colorless solid (133.5 mg, 47.5%).

Synthesis of ***1***·*MeI*. To molecular balance **1** (25.7 mg, 0.0907 mmol) in chloroform (3 mL) was added methyl iodide (115 μL). The solution was stirred at r.t. for 7 days. Evaporation of the solvent yielded an orange solid, which was washed with 3 mL of ether to give **1**·MeI (29.8 mg, 77%). This was recrystallized from chloroform gave orange crystals suitable for X-ray structural analysis; mp 297.6−301.1 °C; IR (KBr) 2929, 2851, 1623, 1505, 1490, 1455, 768, 752 cm^{-1}; ^{1}H NMR (600 MHz, $CDCl_3$) δ 9.25 (d, *J* = 6.0 Hz, 1H), 8.09 (d, *J* = 7.8 Hz, 1H), 7.60−7.62 (m, 1H), 7.31−7.32 (m, 2H), 7.08 (d, *J* = 7.5 Hz, 1H), 6.98−7.02 (m, 2H), 6.89 (d, *J* = 6.8, 1H), 5.23 (dd, *J* = 3.9, 9.8 Hz, 1H), 4.74 (s, 3H), 4.64 (dd, 3.6, 9.6 Hz, 1H), 3.82 (dd, *J* = 9.8, 14.7 Hz, 1H), 3.55 (dd, *J* = 9.6, 14.7 Hz, 1H), 3.33 (dd, *J* = 3.9, 14.7, 1H), 3.25 (dd, *J* = 3.6, 14.7 Hz, 1H); MS (ESI) *m*/*z* 298 (M^+ − I, 100), 299 (M^+ − I + 1, 24); HRMS calcd for $C_{22}H_{20}N$ $[M^+ - I]^+$ 298.1590, found for 298.1586.

Synthesis of ***1***·*MeBr*. To a solution of **1** (26.2 mg, 0.0925 mmol) in chloroform (3 mL) was added methyl bromide by blowing from cylinder for 30 s. The solution was stirred at room temperature for 7 days. Removal of the solvent yielded a solid, which was washed with 3 mL of ether to give **1**·MeBr (27.5 mg, 78.6%). mp 288.3−289.0 °C (recrystallization from $CHCl_3$); IR (KBr) 3033, 2991, 2960, 2929, 2856, 2361, 1626, 1508, 1491, 1456, 1274, 1254, 1171, 1038, 959, 771, 753, 652, 597, 576 cm-1; ^{1}H NMR (600 MHz, $CDCl_3$) δ 9.59 (d, *J* = 5.4 Hz, 1H), 8.00 (d, *J* = 7.8 Hz, 1H), 7.59 (dd, *J* = 7.5, 6.3 Hz, 1H), 7.52 (dd, *J* = 6.6, 2.4 Hz, 1H), 7.37−7.39 (m, 1H), 7.31−7.32 (m, 2H), 7.03 (d, *J* = 6.6 Hz, 1H), 6.97−6.99 (m, 2H), 6.87 (d, *J* = 6.6 Hz, 1H), 5.13 (dd, *J* = 9.9, 3.3 Hz, 1H), 4.76 (s, 3H), 4.59 (dd, *J* = 9.9, 3.3 Hz, 1H), 3.74 (dd, *J* = 15.0, 10.2 Hz, 1H), 3.52 (dd, *J* = 15.0, 10.2 Hz, 1H), 3.29 (dd, *J* = 15.0, 3.6 Hz, 1H), 3.22 (dd, *J* = 15.0, 3.6 Hz, 1H); MS (ESI) *m*/*z* 298 (M^+ − Br, 100); HRMS calcd for $C_{22}H_{20}N$ $[M - Br]^+$ 298.1590, found for 298.1581.

General Procedure for Exchange of Counteranion. To a solution of **1**·MeBr (9.7 mg, 0.026 mmol) in 3 mL of MeOH was added an equimolar amount of a silver salt. The mixture was stirred for 20 min. After precipitated silver bromide was removed by filtration through a Celite, the filtrate was concentrated to give corresponding salts in quantitative yield.

DOI: 10.1021/acs.joc.6b02295
J. Org. Chem. 2016, 81, 11819−11830

1·$MeBF_4$: mp 252.0−254.4 °C (recrystallization from MeOH); IR (KBr) 3099, 3068, 3016, 2951, 2864, 2358, 1626, 1505, 1491, 1456, 1273, 1128, 1056, 773, 754, 652, 601, 577, 522 cm^{-1}; ^1H NMR (600 MHz, $CDCl_3$) δ 8.59 (d, J = 6.0 Hz, 1H), 8.02 (d, J = 7.8 Hz, 1H), 7.57 (dd, J = 7.8, 6.6 Hz, 1H), 7.45 (dd, J = 5.4, 3.0 Hz, 1H), 7.35−7.36 (m, 1H), 7.30 (dd, J = 5.4, 3.0 Hz, 2H), 7.03 (d, J = 6.6 Hz, 1H), 6.95−6.99 (m, 2H), 6.86 (d, J = 6.6 Hz, 1H), 5.02 (dd, J = 9.6, 3.6 Hz, 1H), 4.59 (dd, J = 9.6, 4.2 Hz, 1H), 4.49 (s, 3H), 3.70 (dd, J = 14.7, 9.9 Hz, 1H), 3.50 (dd, J = 14.7, 9.9 Hz, 1H), 3.30 (dd, J = 14.7, 3.9 Hz, 1H), 3.23 (dd, J = 14.7, 3.9 Hz, 1H); MS (ESI) m/z 298 ($M^+ - BF_4$, 100); HRMS calcd for $C_{22}H_{20}N$ $[M - BF_4]^+$ 298.1590, found for 298.1581.

1·$MePF_6$: mp 264.3−267.2 °C (recrystallization from MeOH); IR (KBr) 3014, 2939, 2891, 2857, 2359 1627, 1503, 1489, 1453, 1271, 952, 880, 839, 780, 757, 557 cm^{-1}; ^1H NMR (600 MHz, $CDCl_3$) δ 8.37 (d, J = 6.0 Hz, 1H), 8.04 (d, J = 7.8 Hz, 1H), 7.57 (dd, J = 7.8, 6.6 Hz, 1H), 7.43−7.45 (m, 1H), 7.37−7.38 (m, 1H), 7.29−7.33 (m, 2H), 6.98−7.04 (m, 3H), 6.87 (d, J = 6.6 Hz, 1H), 4.97 (dd, J = 9.6, 3.6 Hz, 1H), 4.60 (dd, J = 9.6, 4.2 Hz, 1H), 4.45 (s, 3H), 3.68 (dd, J = 15.0, 9.6 Hz, 1H), 3.52 (dd, J = 15.0, 9.6 Hz, 1H), 3.31 (dd, J = 15.0, 3.6 Hz, 1H), 3.24 (dd, J = 15.0, 3.6 Hz, 1H); MS (ESI) m/z 298 ($M^+ - PF_6$, 100); HRMS calcd for $C_{22}H_{20}N$ $[M - PF_6]^+$ 298.1590, found for 298.1587.

1·MeOAc: mp 70.7−71.0 °C (recrystallization from $CHCl_3$); IR (KBr) 3395, 3055, 2916, 2855, 2358, 1673, 1557, 1490, 1403, 1012, 1276, 830, 787, 763, 653, 576 cm^{-1}; ^1H NMR (600 MHz, $CDCl_3$) δ 10.01 (d, J = 6.0 Hz, 1H), 7.93 (d, J = 7.8 Hz, 1H), 7.63 (dd, J = 7.8, 6.0 Hz, 1H), 7.40 (dd, J = 5.4, 3.6 Hz, 1H), 7.37 (dd, J = 5.4, 3.0 Hz, 1H), 7.31−7.32 (m, 2H), 6.97−7.00 (m, 3H), 6.86 (dd, J = 6.0, 2.4, 1H), 4.97 (dd, J = 9.6, 3.6 Hz, 1H), 4.72 (s, 3H), 4.55 (dd, J = 9.6, 3.6 Hz, 1H), 3.63 (dd, J = 14.7, 9.9 Hz, 1H), 3.49 (dd, J = 14.7, 9.9 Hz, 1H), 3.28 (dd, J = 15.0, 3.6 Hz, 1H), 3.21 (dd, J = 14.7, 3.9 Hz, 1H); MS (ESI) m/z 298 ($M^+ - OAc$, 100); HRMS calcd for $C_{22}H_{20}N$ $[M - OAc]^+$ 298.1590, found for 298.1587.

Preparation of 1·MeCl by Exchange of a Bromide Anion to a Chloride Anion. A solution of **1**·MeBr (10.1 mg, 0.0267 mmol) in a 1:1 mixture of MeOH and H_2O (1 mL) was passed through ion-exchange resin (AMBERLITE IRA-900). Removal of the solvent to yield **1**·MeCl (8.3 mg, 92.1%). mp 223.7−225.1 °C (recrystallized from $MeOH/H_2O$); IR (KBr) 3033, 2957, 2367, 2344, 1624, 1490, 1457, 1273, 1234, 1172, 1096, 1035, 771, 757, 603, 578, 505 cm^{-1}; ^1H NMR (600 MHz, $CDCl_3$) δ 9.94 (d, J = 5.4 Hz, 1H), 7.97 (d, J = 7.2 Hz, 1H), 7.57−7.60 (m, 1H), 7.49−7.50 (m, 1H), 7.38−7.39 (m, 1H), 7.32−7.36 (m, 2H), 6.97−7.02 (m, 3H), 6.86−6.87 (m, 1H), 5.07 (d, J = 7.2 Hz, 1H), 4.80 (s, 3H), 4.58 (dd, J = 10.2, 3.0 Hz, 1H), 3.70 (dd, J = 14.7, 9.9 Hz, 1H), 3.52 (dd, J = 14.4, 10.2 Hz, 1H), 3.28 (d, J = 15.0 Hz, 1H), 3.20 (dd, J = 14.7, 3.3 Hz, 1H); MS (ESI) m/z 298 ($M^+ - Cl$, 100); HRMS calcd for $C_{22}H_{20}N$ $[M - Cl]^+$ 298.1590, found for 298.1615.

Synthesis of Compound ***5***. A mixture of azaanthracene **6** (0.0930 g, 0.5189 mmol) and 5,6-dimethoxy-1,3-dihydrobenzo[c]thiophene-2,2-dioxide **8** (0.1359 g, 0.5960 mmol) in 1.0 mL of toluene was irradiated with microwave genarator at 280 °C for 4.5 h. After the solution was cooled to room temperature, removal of the solvent left a crude oil. This oily product and the filtered solid were subjected together to silica gel chromatography with hexane: ethyl acetate 1:1 as an eluent to give a crude solid, which was purified by GPC with chloroform yielded **5** as a colorless solid (0.0224 g, 12.6%). mp 171.6−173.0 °C (recrystallization from CH_2Cl_2/CH_3CN); IR (KBr) 3064, 2995, 2940, 2906, 2854, 2832, 2365, 1605, 1589, 1576, 1520, 1451, 1339, 1263, 1202, 1117, 1100, 1007, 815, 760, 657, 580, 547 cm^{-1}; ^1H NMR (400 MHz, $CDCl_3$) δ 8.20 (d, J = 4.0 Hz, 1H), 7.40 (d, J = 7.2 Hz, 1H), 7.26−7.29 (m, 1H), 7.22−7.24 (m, 1H), 7.12−7.14 (m, 2H), 6.95 (dd, J = 7.4, 5.0 Hz, 1H), 6.45 (s, 1H), 6.34 (s, 1H), 4.52 (dd, J = 8.2, 5.6 Hz, 1H), 4.25 (dd, J = 8.2, 5.6 Hz, 1H), 3.74 (s, 3H), 3.73 (s, 3H), 3.37 (dd, J = 14.6, 8.2 Hz, 1H), 3.12−3.28 (m, 3H); ^{13}C NMR (150 MHz, $CDCl_3$); δ 162.7, 146.6, 146.5, 146.4, 142.5, 142.3, 136.8, 134.0, 132.0, 131.6, 127.1, 126.4, 126.4, 126.3, 121.0, 114.1, 113.8, 55.9, 55.8, 48.4, 44.9, 43.9, 43.0; MS (ESI) m/z 344 (M^+ + 1, 100); HRMS calcd for $C_{23}H_{21}O_2N$ $[M + 1]^+$ 344.1650, found for 344.1670.

*Synthesis of 5,6-Dimethoxy-1,3-dihydrobenzo[c]thiophene-2,2-dioxide (**8**)..*[27b,30] We tried to synthesize dimethoxysultine according to the reported method, we could not obtaine the product, but we obtained the isomer **8**. To a solution of 1,2-bis(bromomethyl)-4,5-dimethoxybenzene (1.537 g, 4.744 mmol) in *N*,*N*-dimethylformamide (15 mL) was added sodium hydroxymethanesulfinate (rongalite) and tetrabutylammonium bromide (0.3184 g, 0.9580 mmol) at 0 °C. The mixture was allowed to stir for 6 h at room temperature. Water (100 mL) was added and the mixture was extracted with chloroform for three times. The combined extracts were washed with brine and dried over magnesium sulfate. Removal of the solvent left a crude product, which was subjected to silica gel chromatography with a 10:1 mixture of chloroform and ether to give **8** (0.8337 g, 77.1%) as white crystals: mp 187−195 °C, ^1H NMR (400 MHz, $CDCl_3$) δ 6.77 (s, 2H), 4.32 (s, 4H), 3.88 (s, 6H). IR (KBr) 2990, 2942, 2837, 1610, 1508, 1470, 1448, 1306, 1220, 1134, 1093, 986, 862, 844 cm^{-1}.

Synthesis of ***5***·*MeI.* To a solution of molecular balance **5** (11.3 mg, 0.0510 mmol) in chloroform (3 mL) was added methyl iodide (150 μL). The solution was stirred for 5 days at room temperature. Removal of the solvent yielded an orange solid, which was washed with ether to give **5** (12.8 mg, 80.0%). mp 162.8−165.2 °C (recrystallization from $CHCl_3$); IR (KBr) 3459, 3006, 2935, 2854, 2832, 2364, 1622, 1606, 1517, 1463, 1403, 1337, 1264, 1237, 1201, 1098, 998, 817, 759, 553 cm^{-1}; ^1H NMR (600 MHz, $CDCl_3$) δ 8.95 (d, J = 6.0 Hz, 1H), 8.13 (d, J = 7.8 Hz, 1H), 7.59−7.62 (m, 2H), 7.34−7.36 (m, 1H), 7.25−7.30 (m, 2H), 6.67 (s, 1H), 6.39 (s, 1H), 5.26 (dd, J = 9.9, 3.9 Hz, 1H), 4.75 (s, 3H), 4.60 (dd, J = 9.6, 3.6 Hz, 1H), 3.81 (dd, J = 15.0, 9.6 Hz, 1H), 3.80 (s, 3H), 3.73 (s, 3H), 3.44 (dd, J = 15.0, 9.6 Hz, 1H), 3.27 (dd, J = 15.0, 4.2 Hz, 1H), 3.18 (dd, J = 15.0, 3.6 Hz, 1H); MS (ESI) m/z 358 ($M^+ - I$, 100); HRMS calcd for $C_{24}H_{24}O_2N$ $[M - I]^+$ 358.1802, found for 358.1784.

Synthesis of Compound ***4***. To a solution of molecular balance **1** (27.5 mg, 0.0970 mmol) in chloroform (3 mL) was added *m*-chloroperoxybenzoic acid (34.2 mg, 0.198 mmol). The solution was stirred at room temperature for 26 h. 5% $NaHSO_3$ solution was added to the reaction mixture, and was extracted with $CHCl_3$. Removal of the solvent under reduced pressure yielded a crude oil, which was purified by GPC with chloroform yielded **4** as a white solid (28.9 mg, 99.3%). mp 184.9−186.0 °C (recrystallization from $CHCl_3$); IR (KBr) 3062, 3016, 2941, 2900, 1604, 1489, 1473, 1435, 1343, 1258, 1171, 1032, 893, 809, 758, 643, 608, 521 cm^{-1}; ^1H NMR (400 MHz, $CDCl_3$) δ 7.91 (dd, J = 6.4, 0.8 Hz, 1H), 7.30−7.34 (m, 1H), 7.21−7.28 (m, 1H), 7.16−7.20 (m, 2H), 7.07−7.09 (m, 1H), 6.98 (d, J = 7.2 Hz, 1H), 6.82−6.97 (m, 4H), 5.38 (dd, J = 8.8, 4.0 Hz, 1H), 4.31 (dd, J = 8.8, 4.0 Hz, 1H), 3.57 (dd, J = 14.4, 8.8 Hz, 1H), 3.35 (dd, J = 14.4, 8.8 Hz, 1H) 3.17 (t, J = 4.8 Hz, 1H), 3.13 (t, J = 4.6 Hz, 1H); ^{13}C NMR (150 MHz, $CDCl_3$); δ 152.2, 141.8, 141.5, 140.5, 139.0, 138.6, 136.6, 130.2, 130.1, 127.5, 127.0, 126.9, 126.8, 126.6, 126.1, 124.0, 122.7, 44.4, 44.4, 41.6, 38.3; MS (ESI) m/z 300 (M^+ + 1, 100); HRMS calcd for $C_{21}H_{18}ON$ $[M + 1]^+$ 300.1383, found for 300.1409.

Synthesis of Compound ***2***. Compound **4** (31.2 mg, 0.104 mmol) was carefully added to $POCl_3$ (2 mL), and the reaction mixture was heated at 110 °C for 2 h. After evapolation of the excess $POCl_3$, the residue was poured onto iced-water. The reaction mixture was made alkaline with aqueous NH_3, and extracted with CH_2Cl_2. The extract was dried over magnesium sulfate, and evaporation of the solvent gave an yellow solid, which was purified by silica gel PTLC with a 3:1 mixture of hexane and ethyl acetate as an eluent solvent to yield **2** as a colorless solid (23.2 mg, 70%) with its regioisomer (8.2 mg, 25%). mp 207.2−208.3 °C (recrystallization from $CHCl_3$); IR (KBr) 3058, 3022, 2950, 2900, 2845, 2364, 1558, 1491, 1449, 1402, 1328, 1234, 1158, 1054, 961, 917, 829, 789, 762, 744, 652, 621, 527 cm^{-1}; ^1H NMR (400 MHz, $CDCl_3$) δ 8.05 (d, J = 5.4 Hz, 1H), 7.30−7.32 (m, 2H), 7.17−7.19 (m, 2H), 6.94 (d, J = 5.4 Hz, 1H), 6.89−6.91 (m, 4H), 4.78 (dd, J = 8.8, 4.4 Hz, 1H), 4.53 (dd, J = 8.8, 4.4 Hz, 1H), 3.38−3.47 (m, 2H), 3.12−3.22 (m, 2H); ^{13}C NMR (150 MHz, $CDCl_3$); δ 164.2, 147.0, 142.4, 141.6, 141.3, 139.2, 139.1, 134.8, 130.5, 129.8, 126.8, 126.8, 126.7, 126.6, 126.5, 126.4, 121.6, 48.4, 43.6, 42.7, 40.8; MS (ESI) m/z 318 (M^+ + 1, 100); HRMS calcd for $C_{21}H_{17}NCl_{35}$ $[M + 1]^+$ 318.1044, found for 318.1065.

DOI: 10.1021/acs.joc.6b02295
J. Org. Chem. 2016, 81, 11819−11830

Synthesis of 2·MeI. To a solution of molecular balance **2** (56.8 mg, 0.178 mmol) in chloroform (3 mL) was added methyl iodide (660 μL). The solution was stirred at room temperature for 3 days. Removal of the solvent yielded an orange solid, which was washed with ether to give **2**·MeI (76.4 mg, 87.9%). mp 193.6−194.4 °C (recrystallization from $CHCl_3$); IR (KBr) 3011, 2859, 2364, 1615, 1568, 1489, 1454, 1434, 1266, 1189, 1097, 954, 892, 850, 767, 749, 529 cm^{-1}; ^1H NMR (600 MHz, $CDCl_3$) δ 9.35 (d, J = 6.6 Hz, 1H), 7.58−7.60 (m, 2H), 7.42−7.43 (m, 1H), 7.35−7.37 (m, 2H), 7.00−7.06 (m, 3H), 6.95−6.97 (m, 1H), 5.14 (dd, J = 10.2, 3.0 Hz, 1H), 4.95 (dd, J = 10.2, 3.0 Hz, 1H), 4.71 (s, 3H), 3.80 (dd, J = 14.7, 10.5 Hz, 1H), 3.60 (dd, J = 14.7, 10.5 Hz, 1H), 3.26 (dd, J = 15.0, 3.0 Hz, 1H), 3.19 (dd, J = 15.0, 3.0 Hz, 1H); MS (ESI) m/z 332 (M^+ − I, 100); HRMS calcd for $C_{22}H_{19}NCl$ $[M - I]^+$ 332.1187, found for 332.1201.

Synthesis of Compound 3. To a solution of **2** (50.2 mg, 0.157 mmol) in tetrahydrofuran (2 mL) was added 40% dimethylamine solution (4 mL). The mixture was heated at 150 °C for 9 h by microwave irradiation. After the solvent was removed under reduced pressure, 5% sodium hydrogen carbonate solution was added to the residue. The reaction mixture was extracted with chloroform and the extract was dried over magnesium sulfate. Removal of the solvent left a crude product, which was subjected to silica gel column chromatography by using a 1:1 mixture of hexane and ethyl acetate to give **3** as a colorless solid (30.1 mg, 61.2%). mp 207.0−208.1 °C (recrystallization from $CHCl_3$); IR (KBr) 3010, 2953, 2915, 2879, 2849, 2804, 2365, 1575, 1543, 1490, 1461, 1434, 1415, 1354, 1199, 1024, 946, 827, 804, 768, 752, 661, 595, 548 cm^{-1}; ^1H NMR (400 MHz, $CDCl_3$) δ 8.06 (d, J = 5.6 Hz, 1H), 7.21−7.24 (m, 2H), 7.07−7.10 (m, 2H), 6.82−6.97 (m, 4H), 6.55 (d, J = 5.6 Hz, 1H), 4.66 (dd, J = 7.6, 5.6 Hz, 1H), 4.49 (dd, J = 8.0, 6.0 Hz, 1H), 3.37−3.50 (m, 2H), 3.20−3.30 (m, 2H), 2.85 (s, 6H); ^{13}C NMR (150 MHz, $CDCl_3$) δ 163.8, 157.3, 147.1, 143.0, 142.6, 140.2, 139.6, 130.4, 129.9, 129.2, 127.1, 126.2, 126.2, 126.1, 126.2, 126.0, 110.9, 48.9, 43.9, 43.7, 42.9, 39.4; MS (ESI) m/z 327 (M^+ + 1, 100); HRMS calcd for $C_{23}H_{22}N_2$ $[M + 1]^+$ 327.1856, found for 327.1852.

Synthesis of 3·MeI. To a solution of molecular balance **3** (14.9 mg, 0.0477 mmol) in chloroform (3 mL) was added methyl iodide (60 μL). The solution was stirred at room temperature for 3 days. Removal of the solvent yielded an orange solid, which was washed with ether to give **3**·MeI (20.0 mg, 92.6%). mp 298.2−299.5 °C (recrystallization from $CHCl_3$); IR (KBr) 2998, 2934, 2364, 1631, 1542, 1490, 1424, 1392, 1206, 818, 770 cm^{-1}; ^1H NMR (600 MHz, $CDCl_3$) δ 8.68 (d, J = 7.2 Hz, 1H), 7.43−7.44 (m, 1H), 7.27−7.30 (m, 4H), 7.03−7.08 (m, 3H), 6.89−6.90 (m, 1H), 6.88 (d, J = 7.2 Hz, 1H), 4.83 (dd, J = 9.6, 3.6 Hz, 1H), 4.69 (dd, J = 9.6, 3.6 Hz, 1H), 4.30 (s, 3H), 3.66 (dd, J = 15.0 Hz, 9.6 Hz, 1H), 3.51 (dd, J = 15.0, 9.6 Hz, 1H), 3.27 (s, 6H), 3.25 (dd, J = 15.0, 3.6 Hz, 1H), 3.19 (dd, J = 15.0, 3.6 Hz, 1H); MS (ESI) m/z 341 (M^+ − I, 100); HRMS calcd for $C_{24}H_{25}N_2$ $[M - I]^+$ 341.2012, found for 341.2034.

■ ASSOCIATED CONTENT

Supporting Information

The Supporting Information is available free of charge on the ACS Publications website at DOI: 10.1021/acs.joc.6b02295.

^1H and ^{13}C NMR spectra, X-ray crystallographic data, theoretical study (PDF)

Crystallographic data (CCDC 1419717−1419718 and 1499985−1499988) (CIF)

■ AUTHOR INFORMATION

Corresponding Author

*E-mail: yamada.shinji@ocha.ac.jp.

Notes

The authors declare no competing financial interest.

■ ACKNOWLEDGMENTS

This work was supported by Grant-in-Aid for Scientific Research (C) from MEXT (No. 25410037) and was partly supported by a Grant-in-Aid for Scientific Research on Innovative Areas "Advanced Molecular Transformations by Organocatalysis" from MEXT.

■ REFERENCES

(1) For reviews, see: (a) Dougherty, D. A. *Acc. Chem. Res.* **2013**, *46*, 885−893. (b) Ma, J. C.; Dougherty, D. A. *Chem. Rev.* **1997**, *97*, 1303−1324.

(2) (a) Dougherty, D. A. *Chem. Rev.* **2008**, *108*, 1624−1653. (b) Dougherty, D. A. *J. Org. Chem.* **2008**, *73*, 3667−3673. (c) Scrutton, N. S.; Raine, A. R. C. *Biochem. J.* **1996**, *319*, 1−8. (d) Dougherty, D. A. *Science* **1996**, *96*, 163−167.

(3) Mahadevi, A. S.; Sastry, G. N. *Chem. Rev.* **2013**, *113*, 2100−2138.

(4) (a) Salonen, L. M.; Ellermann, M.; Diederich, F. *Angew. Chem., Int. Ed.* **2011**, *50*, 4808−4842. (b) Meyer, E. A.; Castellano, R. K.; Diederich, F. *Angew. Chem., Int. Ed.* **2003**, *42*, 1210−1250.

(5) For selected examples, see: (a) Yinghe, Z.; Zhonghan, H. *J. Phys. Chem. B* **2013**, *117*, 10540−10547. (b) Zhang, H.; Cui, H. *Langmuir* **2009**, *25*, 2604−2612. (c) Wang, J.; Chu, H.; Li, Y. *ACS Nano* **2008**, *2*, 2540−2546. (d) Pan, D.; Shuna, L.; Ping, W.; Chenxin, C. *Electrochim. Acta* **2007**, *52*, 6534−6547. (e) Fukushima, T.; Aida, T. *Chem. - Eur. J.* **2007**, *13*, 5048−5058. (f) Fukushima, T.; Kosaka, A.; Ishimura, Y.; Yamamoto, T.; Takigawa, T.; Ishii, N.; Aida, T. *Science* **2003**, *300*, 2072−2074.

(6) For selected examples, see: (a) Kim, S.; Huang, J.; Lee, Y.; Duttac, S.; Yooe, H. Y.; Jung, Y. M.; Jho, Y. S.; Zeng, H.; Hwang, D. S. *Proc. Natl. Acad. Sci. U. S. A.* **2016**, *113*, E847−E853. (b) Lim, C.; Huang, J.; Kim, S.; Lee, H.; Zeng, H.; Hwang, D. S. *Angew. Chem., Int. Ed.* **2016**, *55*, 3342−3346. (c) Lu, Q.; Oh, D. X.; Lee, Y.; Jho, Y.; Hwang, D. S.; Zeng, H. *Angew. Chem., Int. Ed.* **2013**, *52*, 3944−3948. (d) Wang, R.; Xie, T. *Chem. Commun.* **2010**, *46*, 1341−1343. (e) Lomadze, N.; Schneider, H. J.; Kato, K. *Angew. Chem., Int. Ed.* **2007**, *46*, 2694−2696.

(7) Tsuzuki, S.; Mikami, M.; Yamada, S. *J. Am. Chem. Soc.* **2007**, *129*, 8656−8175.

(8) For reviews, see: (a) Kennedy, C. R.; Lin, S.; Jacobsen, E. N. *Angew. Chem., Int. Ed.* **2016**, *55*, 12596−12624. (b) Yamada, S.; Fossey, J. S. *Org. Biomol. Chem.* **2011**, *9*, 7275−7281. (c) Yamada, S. *Org. Biomol. Chem.* **2007**, *5*, 2903−2912.

(9) (a) Yamada, S.; Tokugawa, Y. *J. Am. Chem. Soc.* **2009**, *131*, 2098−2099. (b) Yamada, S.; Morimoto, Y.; Misono, T. *Tetrahedron Lett.* **2005**, *46*, 5673−5676. (c) Yamada, S.; Morita, C. *J. Am. Chem. Soc.* **2002**, *124*, 8184−8185.

(10) For reviews, see: (a) Mati, I. K.; Cockroft, S. L. *Chem. Soc. Rev.* **2010**, *39*, 4195−4205. (b) Jennings, W. B.; Farell, B. M.; Malone, J. F. *Acc. Chem. Res.* **2001**, *34*, 885−894.

(11) (a) Paliwal, S.; Geib, S.; Wilcox, C. S. *J. Am. Chem. Soc.* **1994**, *116*, 4497−4498. (b) Kim, E.; Paliwal, S.; Wilcox, C. S. *J. Am. Chem. Soc.* **1998**, *120*, 11192−11193.

(12) Tröger's base derivatives: (a) Adam, C.; Yang, L.; Cockroft, S. L. *Angew. Chem., Int. Ed.* **2015**, *54*, 1164−1167. (b) Yang, L.; Adam, C.; Cockroft, S. L. *J. Am. Chem. Soc.* **2015**, *137*, 10084−10087. (c) Yang, L.; Adam, C.; Nichol, G. S.; Cockroft, S. L. *Nat. Chem.* **2013**, *5*, 1006−1010. (d) Bhayana, B. *J. Org. Chem.* **2013**, *78*, 6758−6762. (e) Cockroft, S. L.; Hunter, C. A. *Chem. Commun.* **2009**, 3961−3963. (f) Fischer, F. R.; Schweizer, W. B.; Diederich, F. *Chem. Commun.* **2008**, 4031−4033. (g) Fischer, F. R.; Bernd, W.; Diederich, F. *Angew. Chem., Int. Ed.* **2007**, *46*, 8270−8273.

(13) Conformation restricted cyclophanes: (a) Fukazawa, Y.; Usui, S.; Tanimoto, K.; Hirai, Y. *J. Am. Chem. Soc.* **1994**, *116*, 8169−8175. (b) Schladetzky, K. D.; Haque, T. S.; Gellman, S. *J. Org. Chem.* **1995**, *60*, 4108−4113.

(14) *N*-arylsuccinimides: (a) Hwang, J.; Li, P.; Smith, M. D.; Shimizu, K. D. *Angew. Chem., Int. Ed.* **2016**, *55*, 1−5. (b) Emenike, B. U.; Bey, S. N.; Bigelowa, B. C.; Chakravartula, S. V. S. *Chem. Sci.* **2016**, *7*, 1401−

DOI: 10.1021/acs.joc.6b02295
J. Org. Chem. 2016, 81, 11819−11830

1407. (c) Hwang, J.; Dial, B. E.; Li, P.; Kozik, M. E.; Smith, M. D.; Shimizu, K. D. *Chem. Sci.* **2015**, *6*, 4358−4364. (d) Maier, J. M.; Li, P.; Hwang, J.; Smith, M. D.; Shimizu, K. D. *J. Am. Chem. Soc.* **2015**, *137*, 8014−8017. (e) Hwang, J.; Li, P.; Carroll, W. R.; Smith, M. D.; Pellechia, P. J.; Shimizu, K. D. *J. Am. Chem. Soc.* **2014**, *136*, 14060−14067. (f) Zhao, C.; Li, P.; Smith, M. D.; Pellechia, P. J.; Shimizu, K. D. *Org. Lett.* **2014**, *16*, 3520−3523. (g) Li, P.; Parker, T. M.; Hwang, J.; Deng, F.; Smith, M. D.; Pellechia, P. J.; Sherrill, C. D.; Shimizu, K. D. *Org. Lett.* **2014**, *16*, 5064−5067.

(15) Propargylic amides: (a) Gardner, R. R.; Christianson, L. A.; Gellman, S. H. *J. Am. Chem. Soc.* **1997**, *119*, 5041−5042. (b) Gardner, R. R.; Mckay, S. L.; Gellman, S. H. *Org. Lett.* **2000**, *2*, 2335−2338.

(16) Triptycenes: (a) Benjamin, M. P.; Gung, W.; Reich, H. J. *J. Org. Chem.* **2005**, *70*, 3641−3644. (b) Benjamin, M. P.; Gung, W.; Barnes, C. L. *J. Org. Chem.* **2008**, *73*, 1803−1808.

(17) Biarylimines: (a) Jennings, W. B.; O'Connell, N.; Malone, J. F.; Boyd, D. R. *Org. Biomol. Chem.* **2013**, *11*, 5278−5291. (b) Jennings, W. B.; McCarthy, N. J.; Kelly, P.; Malone, J. F. *Org. Biomol. Chem.* **2009**, *7*, 5156−5162.

(18) *N*-benzyl pyridinium systems: (a) Rashkin, M. J.; Waters, M. L. *J. Am. Chem. Soc.* **2002**, *124*, 1860−1861. (b) Rashkin, M. J.; Hughes, R. M.; Calloway, N. T.; Waters, M. L. *J. Am. Chem. Soc.* **2004**, *126*, 13320−13325.

(19) Biarylformamides: Muchowska, K. B.; Adam, C.; Mati, I. K.; Cockroft, S. L. *J. Am. Chem. Soc.* **2013**, *135*, 9976−9979.

(20) (a) Aliev, A. E.; Arendorf, J. R.; Pavlakos, I.; Moreno, R. B.; Porter, M. J.; Rzepa, H. S.; Motherwell, W. B. *Angew. Chem., Int. Ed.* **2015**, *54*, 551−555. (b) Motherwell, W. B.; Moise, J.; Aliev, A. E.; Nic, M.; Coles, S. J.; Horton, P. N.; Hursthouse, M. B.; Chessari, G.; Hunter, C. A.; Vinter, J. G. *Angew. Chem., Int. Ed.* **2007**, *46*, 7823−7826.

(21) Preliminary communication, see: Yamada, S.; Yamamoto, N.; Takamori, E. *Org. Lett.* **2015**, *17*, 4862−4865.

(22) A part of this research has been reported in the 25th Symposium on Physical Organic Chemistry held at Sendai, Japan (A book of Abstract, 2P057, 2014). The term "seesaw balance" has been used in there.

(23) Yamada, S.; Kawamura, C. *Org. Lett.* **2012**, *14*, 1572−1575.

(24) Li, P.; Zhao, C.; Smith, M. D.; Shimizu, K. D. *J. Org. Chem.* **2013**, *78*, 5303−5313.

(25) (a) Krapcho, A. P.; Gilmor, T. P. *J. Heterocycl. Chem.* **1999**, *36*, 445−452.

(26) (a) Jarvis, W. F.; Hoey, M. D.; Dittmer, D. C. *J. Org. Chem.* **1988**, *53*, 5750−5756. (b) Hoey, M. D.; Dittmer, D. C. *J. Org. Chem.* **1991**, *56*, 1947−1948.

(27) (a) Jung, F.; Molin, M.; Van den Elzen, R.; Durst, T. *J. Am. Chem. Soc.* **1974**, *96*, 935−936. (b) Schmidt, A. H.; Kircher, G.; Willems, M. *J. Org. Chem.* **2000**, *65*, 2379−2385.

(28) (a) Sisido, K.; Noyori, R.; Nozaki, H. *J. Am. Chem. Soc.* **1962**, *84*, 3562−3566. (b) Sisido, K.; Noyori, R.; Kozaki, N.; Nozaki, H. *Tetrahedron* **1963**, *19*, 1185−1188.

(29) For a review, see: Kappe, C. O. *Angew. Chem., Int. Ed.* **2004**, *43*, 6250−6284.

(30) During attempted preparation of sultine with a dimethoxy group according to the literature, we could not get sultine but we obtained a sulfone as a major product Meng, X.; Xu, Q.; Zhang, W.; Tan, Z.; Li, Y.; Zhang, Z.; Jiang, L.; Shu, C.; Wang, C. *ACS Appl. Mater. Interfaces* **2012**, *4*, 5966−5973.

(31) Yamanaka, H.; Araki, T.; Sakamoto, T. *Chem. Pharm. Bull.* **1988**, *36*, 2244−2247.

(32) (a) Priem, G.; Anson, M. S.; Macdonald, S. J. F.; Pelotier, B.; Campbell, I. B. *Tetrahedron Lett.* **2002**, *43*, 6001−6003. (b) Narayan, S.; Seelhammer, T.; Gawley, R. E. *Tetrahedron Lett.* **2004**, *45*, 757−759.

(33) Hunter, C. A.; Lawson, K. R.; Perkins, J.; Urch, C. J. *J. Chem. Soc. Perkin Trans. 2* **2001**, 651−669.

(34) Fukazawa, Y.; Fujihara, T.; Usui, S. *Tetrahedron Lett.* **1986**, *37*, 5621−5624.

(35) Haasnoot, C. A. G.; de Leeuw, F. A. A. M.; Altona, C. *Tetrahedron* **1980**, *36*, 2783−2792.

(36) Gallivan, J. P.; Dougherty, D. A. *J. Am. Chem. Soc.* **2000**, *122*, 870−874.

(37) Schneider, H.-J. *Angew. Chem., Int. Ed.* **2009**, *48*, 3924−3977.

(38) Mollner, A. K.; Brooksby, P. A.; Loring, J. S.; Bako, I.; Palinkas, G.; Fawcett, W. R. *J. Phys. Chem. A* **2004**, *108*, 3344−3349.

(39) Hunter, C. A.; Low, C. M. R.; Rotger, C.; Vinter, J. G.; Zonta, C. *Proc. Natl. Acad. Sci. U. S. A.* **2002**, *99*, 4873−4876.

(40) Bartoli, S.; Roelens, S. *J. Am. Chem. Soc.* **2002**, *124*, 8307−8315.

(41) (a) Hunter, C. A.; Low, C. M. R.; Rotger, C.; Vinter, J. G.; Zonta, C. *Chem. Commun.* **2003**, 834−835. (b) Cockroft, S. L.; Hunter, C. A. *Chem. Soc. Rev.* **2007**, *36*, 172−188.

(42) Marcus, Y. *Ion Properties*; Marcel Dekker: New York, 1997; Table 3.

(43) For an example, see: Szafran, M.; Bartoszak-Adamska, E.; Koput, J.; Dega-Szafran, Z. *J. Mol. Struct.* **2007**, *844*, 140−156.

DOI: 10.1021/acs.joc.6b02295
J. Org. Chem. 2016, 81, 11819−11830